IAES International Journal of Robotics and Automation (IJRA)
Vol. 15, No. 1, March 2026, pp. 210~221
ISSN: 2722-2586, DOI: 10.11591/ijra.v15i1.pp210-221

Modeling and simulation of an active quarter-car suspension system using a synergetic controller

Dao Trong Dung[1], Trong Nghia Le[2], Alexandr D. Lukyanov[3], Nguyen Xuan Chiem[1]
[1]Department of Automation and Computing Techniques, Le Quy Don Technical University, Hanoi, Vietnam
[2]Research Center for Technical Quality Assurance and Technology Transfer, Le Quy Don Technical University, Hanoi, Vietnam
[3]Department of Automatization of Production Processes, Don State Technical University, Rostov on Don, Russia

Article Info

Article history:

Received Oct 21, 2025
Revised Feb 9, 2026
Accepted Feb 21, 2026

Keywords:

Active suspension system
Lyapunov stability
Nonlinear controller
Sliding-mode controller
Synergetic approach

ABSTRACT

This paper presents the modeling and simulation of an active quarter-car suspension system (AQCSS) designed to enhance operational performance and ride comfort across various road conditions. First, a dynamic quarter-car model was developed, incorporating all the components of AQCSS and road-induced stimuli, based on the Euler–Lagrange method. Subsequently, a synergetic controller is designed by selecting a manifold that meets the system's technical requirements. The proposed controller ensures a balance between ride comfort and road-holding performance by leveraging this manifold design. This control framework enables flexible adjustment of the damping force in real time according to the system states and external excitations. The stability of the closed-loop system is rigorously established through Lyapunov analysis. Numerical simulations are carried out in MATLAB to assess the proposed control law by benchmarking it against a passive suspension configuration and a sliding mode control approach, thereby demonstrating its effectiveness.

Corresponding Author:

Nguyen Xuan Chiem
Department of Automation and Computing Techniques, Le Quy Don Technical University
Hanoi, Vietnam
Email: chiemnx@mta.edu.vn

1. INTRODUCTION

With the rapid advancement of automotive technology, modern vehicle suspension systems have gained increasing attention as a means to enhance ride comfort and vehicle handling performance. Among various subsystems, the suspension system plays a crucial role in ensuring smooth ride quality, road-holding capability, and overall vehicle stability. This system has attracted significant research interest, as presented in studies [1]–[27], due to its ability to adapt dynamic characteristics in real time through the use of advanced sensors and microprocessors for signal acquisition and processing. Such capability allows the suspension system to adjust its behavior according to different road conditions, thereby considerably improving vehicle performance. In general, the performance requirements for active vehicle suspension systems, as discussed in studies [1]–[4], include: i) Ride comfort – isolating the vehicle body from shocks and vibrations induced by road irregularities to ensure passenger comfort; ii) Road holding-eliminating wheel hop to maintain continuous tire-road contact; and iii) Suspension travel limitation constrained by the mechanical structure. However, as reported in [3], it is not feasible to simultaneously satisfy all three performance criteria at their optimal levels, since these objectives tend to be mutually conflicting. To meet these requirements, both passive and active suspension systems have been developed. While passive suspension systems rely solely on springs and dampers with fixed parameters, resulting in limited vibration isolation performance, active

suspension systems can generate controllable forces that allow dynamic adjustment of suspension characteristics to better adapt to varying operating conditions.

Nowadays, autonomous mobile robots are rapidly advancing and being deployed across various domains such as military and industrial applications Platforms like autonomous mobile robots (AMRs), unmanned ground vehicles (UGVs), and remote-sensing robots are typically required to navigate unstructured environments, where challenging terrains, uneven ground, and strong dynamic excitations are common. Consequently, vibrations induced by rough terrain severely affect motion stability, sensor accuracy, actuator lifespan, and payload safety. Therefore, integrating an active suspension system into mobile robotic platforms has become an essential requirement to enhance structural durability, environmental perception capability, and overall system performance [5], [6].

Numerous studies have proposed and applied various control strategies for active suspension systems. For instance, PID control, as presented by Ram *et al.* [4], achieved satisfactory performance but was limited to small operating ranges and was significantly influenced by nonlinear components. In research [7], [8], a linear quadratic regulator (LQR)-based adaptive control was developed; however, its performance remained limited due to the use of a linear controller. Neural network–based control strategies, presented in [9], [11], demonstrated good system performance under model uncertainties, but they suffered from long response times and were difficult to implement in embedded systems. Adaptive control based on backstepping, as proposed by Chen *et al.* [12], yielded impressive results but was constrained by the physical limits of the system. Various sliding mode control (SMC) schemes and their modifications have been reported in [13]–[16], [25], producing favorable results, although the system responses at equilibrium still exhibited oscillations. Robust control approaches were developed in [17]–[19]; however, improvements in control quality and response time are still required. Additionally, fuzzy logic–based control laws have shown promising outcomes in [20], [21], yet the system response time remains relatively long. Adaptive control combined with reinforcement learning, proposed by Kimball *et al.* [22], demonstrated good performance but faced challenges in satisfying the physical constraints of the system. Machine learning–based approaches can alleviate these limitations by exploiting measured feedback signals to refine either the plant model or the control policy itself, as reported in [22]. In particular, study [22] compared several learning-driven control strategies for this system, including adaptive schemes, stability-oriented online learning, and reinforcement learning methods that seek performance improvement through repeated interaction with the system. Furthermore, several works have investigated Lyapunov-based control laws that explicitly account for physical constraints [23], [25]. From a nonlinear control perspective, most existing studies rely on designing a suitable Lyapunov candidate function to ensure closed-loop stability. Traditional controllers based on quadratic Lyapunov functions have proven effective in many scenarios; however, they encounter limitations when applied to systems with strict state constraints. To address this issue, a barrier Lyapunov function (BLF)-based approach has been developed for constrained nonlinear control problems, as presented in [24]. The key feature of this method is the use of a candidate Lyapunov function that approaches infinity as the system state nears the constraint boundary, thereby ensuring that the constraints are never violated. The BLF-based approach enables the design of more stable and robust control laws, even when the initial system states are close to the constraint boundaries. Although the aforementioned studies have successfully reduced system oscillations, most have not explicitly incorporated the physical constraints among the system state variables.

Another widely adopted approach for controlling complex mechatronic systems is the application of synergetic control theory, as presented in the literature [28]–[30]. The core concept involves designing a control framework capable of "integrating" multiple sub controllers, each responsible for a specific objective within the closed-loop system, based on the dynamics of individual control loops [28], [29]. In synergistic control theory, desired values are expressed as invariants that can be constructed based on the physical nature of the system, not just on mathematical models; this is an advantage over other control methods. Several studies have proposed synergetic controllers for active suspension systems and reported promising results. For instance, in study [30], a synergetic controller was developed based on a particular manifold while accounting for the physical constraints of the system. However, an in-depth analysis of the overall system stability under this control law has not yet been conducted.

This paper focuses on the modeling and simulation of an active quarter-car suspension system (AQCSS) employing a synergetic control strategy. The system dynamics are derived via the Euler–Lagrange formulation, which explicitly accounts for the coupling among the mechanical elements as well as road-induced disturbances. The synergetic controller proposed in this study is designed based on the selection of a novel manifold capable of satisfying the system's technical requirements. This approach offers the advantage of integrating technical requirements into the control law, thereby significantly enhancing the stability of the active suspension system under various operating conditions. The system stability under the proposed control law is rigorously proven using Lyapunov's method, and MATLAB simulation results demonstrate that the proposed controller significantly outperforms traditional passive suspension systems. The remainder of the paper is organized as follows: Section 2 presents the modeling methodology for the constrained active

suspension system; Section 3 details the synthesis of the constrained synergetic controller, stability analysis under external disturbances, and the design of an SMC controller; Section 4 provides simulation scenarios to validate the effectiveness of the proposed control law; and Section 5 concludes the paper.

2. DYNAMIC MODELING

In this study, the AQCSS is illustrated in Figure 1, which is widely adopted in research [1]–[7]. The model considers two masses: The sprung mass $m_s = m + \delta_{m_s}$, representing the vehicle body mass (m) together with the passengers and payload (δ_{m_s}) and the unsprung mass m_u associated with the wheel-axle assembly. The suspension system consists of a spring–damper unit defined by the parameters k_{1s}, k_{2s}, c_{1s}, and c_{2s}. Here, k_{1s} and k_{2s} denote the linear and cubic stiffness coefficients, while c_{1s} and c_{2s} denote the linear and cubic damping coefficients, respectively, which together describe the nonlinear characteristics of the suspension system. The tire is modeled with stiffness k_t and damping c_t; nevertheless, in numerous studies [1], [2], it is commonly simplified as a purely linear elastic element represented only by the stiffness parameter k_t. The control variable u represents the force generated by the active suspension actuator, acting on the sprung mass, while an equal and opposite reaction force $-u$ acts on the unsprung mass. The system states are represented by the vertical displacements of the sprung mass z_s, the unsprung mass z_u, and the road excitation z_r.

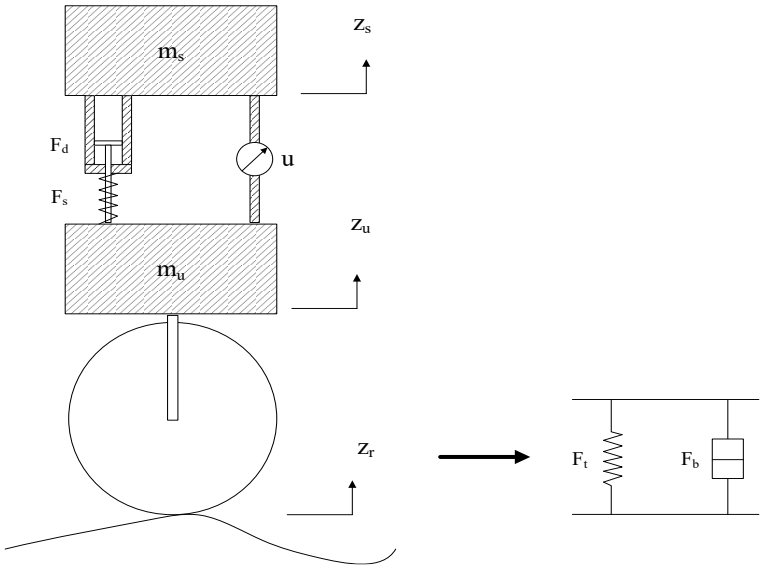

Figure 1. Model of an AQCSS

In practical systems, either electric motor actuators or hydraulic actuators are commonly employed to generate the control force u, which acts simultaneously on both the sprung mass (m_s) and the unsprung mass (m_u) [31], [32]. The displacements of the sprung and unsprung masses are typically measured using commercial linear variable differential transformers, linear potentiometers, optical encoders, ultrasonic sensors, or laser-based sensors in laboratory-scale platforms. The velocities of these masses are obtained either from direct velocity sensors, accelerometers, or indirectly estimated from the measured displacement signals described above [31]–[33].

The total kinetic energy of the quarter-car model is obtained by summing the contributions of the sprung and unsprung masses, and is written as (1).

$$T = \frac{1}{2} m_s \dot{z}_s^2 + \frac{1}{2} m_u \dot{z}_u^2 \tag{1}$$

For modeling convenience, the tire is assumed to maintain continuous contact with the road. Consequently, the potential energy formulation accounts for the elastic deformation of the spring, including the cubic nonlinear stiffness effect that occurs during compression, and is expressed as (2).

$$V = \frac{1}{2}k_{1s}(z_s - z_u)^2 + \frac{1}{4}k_{2s}(z_s - z_u)^4 + \frac{1}{2}k_t(z_u - z_r)^2 \quad (2)$$

The system Lagrangian is defined as $L = T - V$, where T and V represent the kinetic and potential energies, respectively. The damping-related energy loss is modeled using the Rayleigh dissipation function:

$$D = \frac{1}{2}c_{1s}(\dot{z}_s - \dot{z}_u)^2 + \frac{1}{4}c_{2s}(\dot{z}_s - \dot{z}_u)^4 + \frac{1}{2}c_t(\dot{z}_u - \dot{z}_r)^2 \quad (3)$$

For each generalized coordinate $q = [z_s, z_u]^T$, the Euler–Lagrange equation with a dissipation term D and external forces is given by (4):

$$\frac{d}{dt}\left(\frac{\partial L}{\partial \dot{q}_i}\right) - \frac{\partial L}{\partial q_i} + \frac{\partial D}{\partial \dot{q}_i} = Q_i \quad (4)$$

Here, Q_i represents the generalized external forces, including the control input u in the present formulation.

After substituting z_s and z_u, the governing equations of the active quarter-car suspension are obtained in the form of the differential equations of (5),

$$\begin{cases} m_s\ddot{z}_s + F_d + F_s = u \\ m_u\ddot{z}_u - F_d - F_s + k_t(z_u - z_r) + c_t(\dot{z}_u - \dot{z}_r) = -u \end{cases} \quad (5)$$

where

$$F_s = k_{1s}(z_s - z_u) + k_{2s}(z_s - z_u)^3; \quad F_d = c_{1s}(\dot{z}_s - \dot{z}_u) + c_{2s}(\dot{z}_s - \dot{z}_u)^2; \quad (6)$$

In the AQCSS, the vertical road profile z_r is practically difficult to measure, and designing a reliable observer for such an unmeasurable disturbance is inherently challenging. Consequently, during the synthesis of the control law, the term involving this variable is regarded as an external disturbance. Let the state variables be defined as: $x_1 = z_s, x_2 = \dot{z}_s, x_3 = z_u, x_4 = \dot{z}_u$. Then, the system (5) can be represented in state-space form as (7),

$$\begin{cases} \dot{x}_1 = x_2 \\ \dot{x}_2 = \left(m + \delta_{m_s}\right)^{-1}(-F_d - F_s + u) \\ \dot{x}_3 = x_4 \\ \dot{x}_4 = {m_u}^{-1}(F_d + F_s - k_t x_3 - c_t x_4 - u + d(t)) \end{cases} \quad (7)$$

where $d(t) = k_t z_r + c_t \dot{z}_r$.

The goal of this study is to synthesize a control law u in the system (7) based on manifold composite control theory that ensures the AQCSS meets the following requirements:

– The main control objective is that the controller must stabilize the vertical motion of the sprung mass m_s within the mechanical limits of the system when there is a change in the system parameters and the impact of various types of road surface disturbances:

$$\lim_{t\to\infty}(z_s(t)) \to 0 \quad (8)$$

– Define the relative suspension deviation (RSD) as the suspension deflection normalized by the maximum vibration-space limit z_{max}. This quantity must satisfy $RSD < 1$, which can be expressed as (9):

$$RSD = \frac{z_s - z_u}{z_{max}} < 1 \quad (9)$$

– Continuous tire–road contact must be maintained while avoiding excessive tire loads. Accordingly, the relative tire force (RTF), defined as the tire dynamic load normalized by the static load, should satisfy $RTF < 1$:

$$RTF = \frac{k_t(z_u - z_r) + c_t(\dot{z}_u - \dot{z}_r)}{(m_s + m_u)g} < 1 \quad (10)$$

3. SYNTHESIS OF CONTROL LAWS FOR AN ACTIVE QUARTER-CAR SUSPENSION SYSTEM

3.1. Synergetic control law design

In synergetic control theory, the set of control objectives or performance criteria is defined in the form of a system of invariants. For electromechanical systems, studies [28], [29] distinguished three main types of invariants: technological, electromagnetic, and energy invariants. The technological invariant defines the target static or dynamic condition of the system associated with a given technological task to achieve mechanical motion. The electromagnetic invariant is selected to ensure the stable operation of electrical and magnetic variables within the actuator. Finally, the energy invariant expresses the relationships between system variables that reflect optimal energy conversion conditions, particularly those minimizing energy losses during operation.

The choice of invariants is essential for control system synthesis and is based on the technological requirements and the number of physical control inputs. For an active quarter-car suspension system, these control channels correspond to the vertical displacement amplitudes of the two mass centers, m_s and m_u. For this system, the invariant manifold must accurately reflect the requirements imposed on the control law and must exclude any state variables that are not directly measurable. Based on the above analysis, together with the control requirements for the system presented in section 2, and relying on the invariant manifold–based synergetic control theory, one can select the form for system as in (7).

$$\psi = x_2 + k_1\left(x_1 + \frac{k_2}{2} ln\left(\frac{Z_{max}+x_1-x_3}{Z_{max}-(x_1-x_3)}\right)\right) \tag{11}$$

where k_1, $k_2 > 0$ are positive constants.

When the system operates on the manifold defined by (11), *i.e.*, when $\psi=0$, it follows that:

$$x_2 + k_1\left(x_1 + \frac{k_2}{2} ln\left(\frac{Z_{max}+x_1-x_3}{Z_{max}-(x_1-x_3)}\right)\right) = 0 \Rightarrow \frac{1}{2} ln\left(\frac{Z_{max}+x_1-x_3}{Z_{max}-(x_1-x_3)} = \frac{-x_2-k_1x_1}{k_1k_2}\right)$$

Accordingly, by applying the inverse of the tanh function, we obtain (12).

$$x_1 - x_3 = z_{max}\, tanh\left(\frac{x_2+x_1k_1}{k_1k_2}\right) \tag{12}$$

Since the hyperbolic tangent function is bounded, from the RSD requirement (9) it can be inferred that the damping travel is limited by the maximum allowable value z_{max}. Assuming k_2 is a small positive constant and as the system evolves on manifold ψ=0, we obtain (13).

$$x_2 \approx -k_1x_1 \tag{13}$$

From (13), combined with the first equation of the system (7), we get a first-order differential equation in x_1. It is easy to prove that with $k_1>0$, $x_1 \to 0$ when $t\to\infty$ satisfies condition (8). Since this equation is autonomous, according to (12), we can conclude that when condition (9) is satisfied, the displacement of the suspended mass m_s becomes negligible regardless of the change in the road surface.

Following the analytical design of aggregated regulators methodology for controller synthesis, the invariant manifold (9) satisfies the differential constraint:

$$\dot{\psi} + T_1\psi = 0 \tag{14}$$

where $T_1>0$ is a design time constant that governs the convergence speed of the system trajectories toward the manifold $\psi=0$. Based on the solution of (12) and taking into account the plant model (7), and under the assumption that $\delta_{ms} = 0$, the synergetic control law can be derived as (15).

$$\dot{x}_2 + k_1\left(\dot{x}_1 + k_2\frac{z_{max}(x_2-x_4)}{z_{max}^2-(x_1-x_3)^2} + T_1\psi = 0\right) \tag{15}$$

Substituting into the second equation of system (7), we obtain (16).

$$m^{-1}(-F_d - F_s + u) + k_1\left(\dot{x}_1 + k_2\frac{z_{max}(x_2-x_4)}{z_{max}^2-(x_1-x_3)^2} + T_1\psi = 0\right) \tag{16}$$

Hence,

$$u = F_d + F_s - mk_1\left(x_2 + k_2\frac{z_{max}(x_2-x_4)}{z_{max}^2-(x_1-x_3)^2} - mT_1\psi\right) \quad (17)$$
$$+Stability\ Analysis$$

We begin by assessing the stability of the sprung mass dynamics m_s governed by control law (17) and the first two equations in (7). A Lyapunov candidate is then introduced to ensure that the trajectories converge to the manifold ψ=0.

$$V_s = 0.5\psi^2 \quad (18)$$

Taking the time derivative, these yields (19).

$$\dot{V}_s = \psi\left(\dot{x}_2 + k_1\left(x_2 + k_2\frac{z_{max}(x_2-x_4)}{z_{max}^2-(x_1-x_3)^2}\right)\right) \quad (19)$$

Substituting (17) and (7) into (19), we obtain (20).

$$\dot{V}_s = \psi\left(\frac{1}{m_s}\left(-mk_1\left(x_2 + k_2\frac{z_{max}(x_2-x_4)}{z_{max}^2-(x_1-x_3)^2}\right) - mT_1\psi\right) + k_1\left(x_2 + k_2\frac{z_{max}(x_2-x_4)}{z_{max}^2-(x_1-x_3)^2}\right)\right) \quad (20)$$

Hence,

$$\dot{V}_s = \frac{k_1\delta_{m_s}}{m_s}\left(x_2 + k_2\frac{z_{max}(x_2-x_4)}{z_{max}^2-(x_1-x_3)^2}\right)\psi - \frac{m}{m_s}T_1\psi^2 \quad (21)$$

When there is no variation in the mass $\delta_{m_s} = 0$, we obtain $\dot{V} = -T_1\psi^2 \leq 0$, and thus the system is globally asymptotically stable. When $\delta_{m_s} \neq 0$, applying the Young's inequality, we have (22).

$$\dot{V}_s \leq -\frac{2mT_1-k_1\delta_{m_s}}{2m_s}\psi^2 + \frac{k_1\delta_{m_s}}{2m_s}\left(x_2 + k_2 z_{max}\frac{(x_2-x_4)}{z_{max}^2-(x_1-x_3)^2}\right)^2 \quad (22)$$

It is easy to observe that, under $\delta_{m_s} < 2mT_1/k_1$, a sufficient condition to ensure $\dot{V}_s \leq \Delta_s$ is given by (23).

$$\left(x_2 + k_2 z_{max}\frac{(x_2-x_4)}{z_{max}^2-(x_1-x_3)^2}\right)^2 \leq \Delta_s\frac{2m_s}{k_1\delta_{m_s}} \quad (23)$$

This implies that when x is sufficiently far from the origin with a positive Δ_s, we obtain $\dot{V}_s \leq 0$. Consequently, the sprung-mass subsystem m_s is stabilized in a neighborhood of the equilibrium point, namely within a ball of radius Δ_s centered at the origin.

The second step is to establish the stability of system (7). To ensure all the necessary asymptotically stable states of the system, the Lyapunov function is constructed based on the V_s function in the first step, and adds the positive definite component of x_4.

$$V = V_s + 0.5x_4^2 \quad (24)$$

Taking the time derivative, these yields (25).

$$\dot{V} = \psi\left(\dot{x}_2 + k_1\left(x_2 + k_2\frac{z_{max}(x_2-x_4)}{z_{max}^2-(x_1-x_3)^2}\right)\right) + x_4\dot{x}_4 \quad (25)$$

Substituting (7) and (13) into (20), we obtain (26).

$$\dot{V} = \dot{V}_s + \frac{1}{m_u}x_4\left(-k_t x_3 - c_t x_4 + mk_1\left(x_2 + k_2\frac{z_{max}(x_2-x_4)}{z_{max}^2-(x_1-x_3)^2}\right) + mT_1\psi + d(t)\right) \quad (26)$$

By simplification, we obtain (27).

$$\dot{V} = \dot{V}_s - \left(\frac{c_t}{m_u} + \frac{mk_1k_2}{z_{max}^2-(x_1-x_3)^2}\right)x_4^2 + \frac{-k_tx_3+mk_1\left(x_2+k_2\frac{z_{max}x_2}{z_{max}^2-(x_1-x_3)^2}\right)+d(t)}{m_u}x_4 \quad (27)$$

Based on the analysis in the first step, the suspended mass system m_s is asymptotically stable, *i.e.*, $x_1 \to 0$ and $x_2 \to 0$. As a result, equation (27) can be recast into the form of (28).

$$\dot{V} = \dot{V}_s - \left(\frac{c_t}{m_u} + \frac{mk_1k_2}{z_{max}^2-x_3^2}\right)x_4^2 + \frac{-k_tx_3+d(t)}{m_u}x_4 \quad (28)$$

By applying the Young's inequality, we obtain (29).

$$\dot{V} = \dot{V}_s - \left(\frac{c_t}{m_u} + \frac{mk_1k_2}{z_{max}^2-x_3^2} - \frac{1}{m_u}\right)x_4^2 + \frac{1}{m_u}(-k_tx_3 + d(t))^2 \quad (29)$$

Under the practical condition that the road surface irregularities are bounded, x_3 is constrained according to (9) when the invariant manifold (8) is satisfied, *i.e.*, $(-k_tx_3 + d(t))^2 < \Delta$. To ensure $\dot{V} \leq 0$, this implies that

$$(-k_tx_3 + d(t))^2 \leq -\left(c_t - 1 + \frac{m_umk_1k_2}{z_{max}^2-x_3^2}\right)x_4^2 \quad (30)$$

It is straightforward to observe that when x_4 is sufficiently far from the origin, condition (30) holds. This implies that system (7) under control law (17) will move toward a neighborhood of the origin when it is outside the region Δ. Once the trajectories enter Δ, the system will remain within this region and all state variables will converge to zero. Moreover, with a sufficiently small Δ, the steady-state tracking errors still satisfy the required performance specifications and control objectives. In order to provide an additional comparison and assess the proposed control law (17), we design a SMC for system (7).

3.2. Sliding mode control law design

The design of the SMC controller for suspension systems has been presented in various studies [25]. Sliding-mode control is a robust nonlinear control approach capable of maintaining stable control performance even in the presence of disturbances and parameter uncertainties. The main idea of SMC is to construct a sliding surface such that, once the system trajectories reach and remain on this surface, the system exhibits the desired dynamics and stability is guaranteed. The SMC design method used in this section follows the approach reported in [25]. The control objective of the active suspension system is to ensure that the actual suspension deflection $y=x_1-x_3$ quickly and accurately tracks its desired reference y_d. Based on the system equations in (7) and following the above-mentioned study, the output tracking error of the system is defined as:

$$e = y_d - x_1 + x_3 \quad (31)$$

The controller sliding surface s is defined as:

$$s = \ddot{e} + c_2\dot{e} + c_1e \quad (32)$$

where $c_1>0$ and $c_2>0$ are positive constants ensuring asymptotic stability on the sliding surface.

The sliding-mode control input is composed of two parts: the equivalent term u_{eq} and the switching term u_{sw}. The equivalent control compensates the nominal dynamics so that the motion remains on the sliding manifold; it is obtained by enforcing $\dot{s} = 0$. In contrast, the switching control drives the trajectories toward the manifold, ensuring the reaching condition. Accordingly, the SMC law is given by (33):

$$u = u_{eq} + u_{sw} \quad (33)$$

The components of the control law in (33) are given by (34):

$$u_{eq} = -\frac{1}{\beta}(\dddot{y}_d + c_2\ddot{y}_d + c_1\dot{y}_d + \alpha_1x_1 + \alpha_2x_2 + \alpha_3x_3 + \alpha_4x_4 + \alpha_5x_5)$$
$$u_{sw} = -\frac{1}{\beta}K\,sgn(s) \quad (34)$$

In this formulation, the variable x_5 is introduced to represent the state of the actuator, and the parameters α_i $(i = 1 \ldots 5)$ are also determined according to the expressions provided in the same study [25].

4. NUMERICAL SIMULATION RESULTS AND DISCUSSION

To validate the proposed control strategy, we compare three cases in simulation: the passive suspension system (PSS), sliding mode control (SMC), and synergetic control ($Syn.C$). The quarter-car model parameters used in the simulations are given in Table 1 [3]. Controller parameters are tuned following the stability conditions derived earlier. All proposed controller parameters T_1, k_1, and k_2 are positive constants. According to the analysis of (11) and (14), k_2 is a small positive constant and is therefore chosen as k_2=0.005. The parameter k_1=30 mainly affects the settling time of the system, and it is selected to ensure fast stability in accordance with (11). Similarly, T_1=10 is chosen to guarantee an appropriate settling time for the overall system, thereby ensuring its stability. For the SMC controller selected according to the referenced study, the parameters are chosen as follows: K=2, c_1=8, c_2=4 and the remaining parameters are computed using the formulas that depend on the system parameters reported in [25]. The simulation program was implemented in MATLAB using the forward Euler method with a sampling time of $\Delta t = 0.001\ s$.

Table 1. AQCSS model parameters

Parameter	Value	Units
m_s	600	kg
m_u	60	kg
k_{1s}	18000	N/m
k_{2s}	1000	N/m^3
c_{1s}	2500	Ns/m
c_{2s}	2200	Ns^2/m^2
c_t	1000	Ns/m
k_t	200000	N/m
z_{max}	0.15	m

4.1. Scenario 1 – Road disturbance: Bump input

For the first simulation scenario, a bump-type road profile is used as the excitation and is described by (35):

$$z_r(t) = \begin{cases} d(t); & else \\ -a(t-3.5)^3 + b(t-3.5)^2 + d(t); & 3.5 \le t < 5 \\ a(t-6.5)^3 + b(t-6.5)^2 + d(t); & 5 \le t < 6.5 \\ a(t-8.5)^3 - b(t-8.5)^2 + d(t); & 8.5 \le t < 10 \\ -a(t-11.5)^3 - b(t-11.5)^2 + d(t); & 10 \le t < 11.5 \end{cases} \quad (35)$$

where $a = 0.0592$, $b = 0.1332$, and $d(t) = 0.002(sin(2\pi t) + sin(7.5\pi t))\ (m)$ represents a sinusoidal disturbance.

The simulation results of the suspension system's response are illustrated in Figure 2. The time-domain response of the suspension mass displacement is compared in Figure 2(a). According to the oscillation responses shown in the figure, the PSS shows the largest displacement amplitude of the suspension mass, reaching approximately $\pm 0.12\ m$. In contrast, the system using the SMC controller maintains the amplitude within $\pm 0.02\ m$, while the system with the $Syn.C$ controller continues to reduce the amplitude to approximately $\pm 0.017\ m$. This demonstrates that the proposed active control scheme $Syn.C$ significantly reduces the vibration amplitude of the suspension mass. Regarding the working space of the AQCSS, the system must maintain its deflection within permissible limits. As illustrated in Figure 2(b), the RSD of the AQCSS with the $Syn.C$ controller is within ± 0.6, while the RSD of the SMC controller is always within ± 0.7. This result shows that both controllers ensure the condition (9). This means that the system ensures safe operation within its mechanical limits. Figure 2(c) shows that the RTF of PSS, SMC, and $Syn.C$ are all less than 1 (10), indicating that the contact between the tire and the road surface is well maintained, thus improving stability and safety during control. However, the RTF of the $Syn.C$ control law has the highest value at certain times, indicating that this control law exhibits a strong response to disturbances, enabling the system to quickly return to its initial position. The control signals of the AQCSS according to the SMC and $Syn.C$ control laws are presented in Figure 2(d). Both control strategies generate two main control pulses with an amplitude of approximately $\pm 1900\ N$ when road disturbances occur. Nevertheless, compared with SMC, the $Syn.C$ scheme achieves similar performance with a marginally reduced control amplitude, supporting the effectiveness of the proposed method.

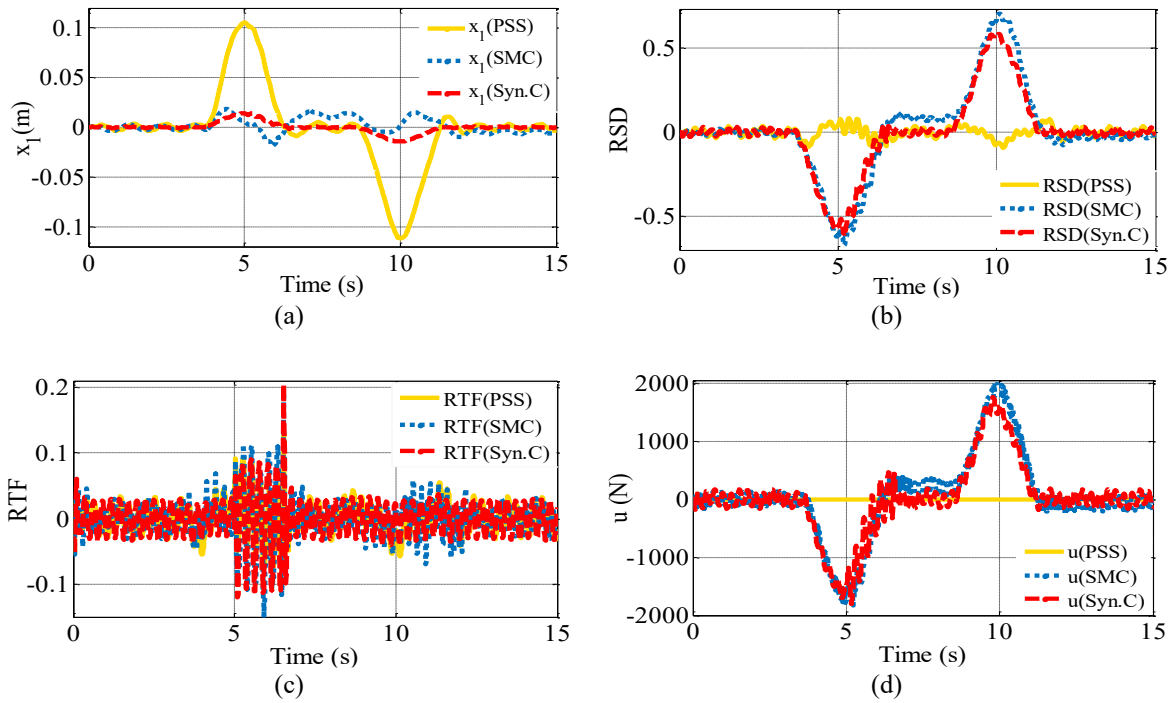

Figure 2. System response in the scenario 1: (a) vertical motion of the sprung mass m_s, (b) the relative suspension deviation, (c) the relative tire force, and (d) control signal in the active suspension system

4.2. Scenario 2 – Road step excitation

In the second scenario, the bump-induced road excitation is described by (36).

$$z_r(t) = \begin{cases} 0.05(1 - cos(16\pi t)), 0 \le t \le 0.025 \\ 0, t > 0.025 \end{cases}, \quad (36)$$

The simulation outcomes for scenario 2 highlight clear differences among the three cases: the active suspension with the $Syn.C$ law, the system governed by the SMC law, and the passive suspension, as summarized in Table 2 and illustrated in Figure 3. As shown in Figure 3(a), the vertical displacement of the sprung mass is attenuated much more rapidly under $Syn.C$ than in the passive case, leading to smaller peak amplitudes and a shorter settling time, as shown in Table 2. This confirms the superior ability of the $Syn.C$ controller in stabilizing the system's suspended mass compared to the SMC controller. Figure 3(b) illustrates RSD, showing that the results indicate all three systems ensure the condition (9). This demonstrates the system's ability to operate within mechanical limits without failure. Figure 3(c) shows the system's RTF, where the system's RTF for both passive and active control always remains below 1, demonstrating that contact between the tire and the road surface is maintained at all times, thus ensuring good traction. Finally, Figure 3(d) presents the control force u, where the $Syn.C$ control law is within $\pm 120\ N$, but rapidly decreases to 0. When disturbances appear, it shows that the $Syn.C$ controller provides a strong corrective effect during the transition phase to effectively suppress oscillations, while gradually reducing energy consumption as the system approaches a steady state. Conversely, although the SMC control signal exhibits a smaller oscillation amplitude, it continues to oscillate around the equilibrium point due to the characteristics of this controller. Overall, the simulations indicate that the proposed $Syn.C$ controller provides rapid, non-oscillatory settling, enhances ride comfort and dynamic stability, and respects the drivetrain constraints.

Table 2. The performance indices evaluating the position response of the m_s

Parameter	PSS	SMC	*Syn.C*	Units
Settling time	1.9	1.8	0.9	s
Overshoot	6×10^{-4}	6×10^{-4}	5.1×10^{-4}	m
Undershoot	-17.3×10^{-4}	-11.1×10^{-4}	-9×10^{-4}	m
Steady-state error	0	0	0	m

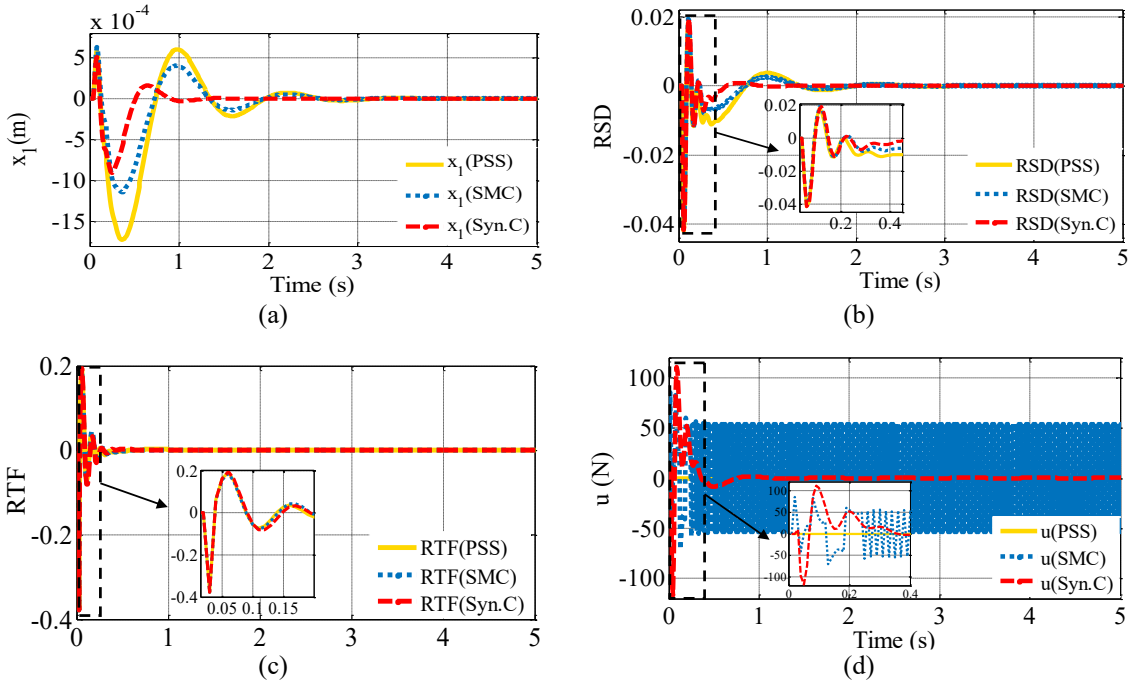

Figure 3. System response in the scenario 2: (a) vertical motion of the sprung mass m_s, (b) the relative suspension deviation, (c) the relative tire force, and (d) control signal in the active suspension system

5. CONCLUSION

This study develops and evaluates a synergetic control scheme for an active quarter-car suspension through modeling, controller design, and numerical simulation. The governing dynamics are derived using the Euler–Lagrange formulation, which captures the nonlinear behavior of the spring–damper elements and the coupling between mechanical components under road-induced excitations. The synergetic controller is constructed to meet the system objectives by balancing the key performance requirements of the active suspension. To this end, an appropriate control manifold is introduced in accordance with the physical constraints of the system. The proposed law first drives the states to the manifold and then ensures self-stabilization. Closed-loop stability in the presence of external disturbances and parameter uncertainties is established via Lyapunov analysis. Simulation outcomes show that the proposed synergetic controller provides noticeable performance gains over both the SMC-based active suspension and the passive configuration, including shorter settling times under different road profiles. Nevertheless, the controllers have not yet been implemented on a real experimental setup. Future work will therefore focus on hardware-in-the-loop implementation to assess feasibility and real-time behavior. Furthermore, to enhance robustness under measurement noise, adaptive control techniques will be investigated, and neural networks or state observers will be considered to estimate the noise component.

FUNDING INFORMATION

This work received no external funding.

AUTHOR CONTRIBUTIONS STATEMENT

This journal uses the Contributor Roles Taxonomy (CRediT) to recognize individual author contributions, reduce authorship disputes, and facilitate collaboration.

Name of Author	C	M	So	Va	Fo	I	R	D	O	E	Vi	Su	P	Fu
Dao Trong Dung	✓	✓	✓	✓		✓	✓	✓		✓			✓	
Trong Nghia Le						✓		✓		✓				✓
Alexandr D. Lukyanov		✓			✓				✓					✓
Nguyen Xuan Chiem	✓	✓		✓	✓		✓	✓	✓	✓	✓	✓	✓	✓

C : **C**onceptualization
M : **M**ethodology
So : **So**ftware
Va : **Va**lidation
Fo : **Fo**rmal analysis
I : **I**nvestigation
R : **R**esources
D : **D**ata Curation
O : Writing - **O**riginal Draft
E : Writing - Review & **E**diting
Vi : **Vi**sualization
Su : **Su**pervision
P : **P**roject administration
Fu : **Fu**nding acquisition

CONFLICT OF INTEREST STATEMENT

Authors state no conflict of interest.

DATA AVAILABILITY

The data presented in this study are available on request from the corresponding author.

REFERENCES

[1] W. Sun, H. Gao, and P. Shi, *Advanced control for vehicle active suspension systems*, vol. 204. Cham: Springer International Publishing, 2020. doi: 10.1007/978-3-030-15785-2.

[2] S. Kashem, R. Nagarajah, and M. Ektesabi, *Vehicle suspension systems and electromagnetic dampers*. Singapore: Springer Singapore, 2018. doi: 10.1007/978-981-10-5478-5.

[3] M. C. Bernardes, B. V. Adorno, P. Poignet, and G. A. Borges, "Robot-assisted automatic insertion of steerable needles with closed-loop imaging feedback and intraoperative trajectory replanning," *Mechatronics*, vol. 23, no. 6, pp. 630–645, Sep. 2013, doi: 10.1016/j.mechatronics.2013.06.004.

[4] S. S. Ram, C. Kumar, R. Saravanakumar, and D. Banjerdpongchai, "System identification and robust PID controller tuning of quarter car suspension system using hybrid optimization techniques," *Scientific Reports*, vol. 15, no. 1, p. 24195, Jul. 2025, doi: 10.1038/s41598-025-10213-9.

[5] W. Szerszeń and P. D. Domański, "Active suspension system for mobile robot: design and analysis," *Nonlinear Dynamics*, vol. 113, no. 19, pp. 25661–25682, Oct. 2025, doi: 10.1007/s11071-025-11474-9.

[6] J. Gao, Y. Li, J. Jin, Z. Jia, and C. Wei, "Design, analysis and control of tracked mobile robot with passive suspension on rugged terrain," *Actuators*, vol. 14, no. 8, p. 389, Aug. 2025, doi: 10.3390/act14080389.

[7] M. Karahan, "Modeling and simulation of an active quarter car suspension with a robust LQR controller under road disturbance and parameter uncertainty," *arXiv:2508.02906*, 2025, doi: 10.48550/arXiv.2508.02906.

[8] T. Abut and E. Salkim, "Control of quarter-car active suspension system based on optimized fuzzy linear quadratic regulator control method," *Applied Sciences*, vol. 13, no. 15, p. 8802, Jul. 2023, doi: 10.3390/app13158802.

[9] L. Liu, X. Li, Y.-J. Liu, and S. Tong, "Neural network based adaptive event trigger control for a class of electromagnetic suspension systems," *Control Engineering Practice*, vol. 106, p. 104675, Jan. 2021, doi: 10.1016/j.conengprac.2020.104675.

[10] V. S. Deshpande, P. D. Shendge, and S. B. Phadke, "Nonlinear control for dual objective active suspension systems," *IEEE Transactions on Intelligent Transportation Systems*, vol. 18, no. 3, pp. 656–665, Mar. 2017, doi: 10.1109/TITS.2016.2585343.

[11] F. Zhao, S. S. Ge, F. Tu, Y. Qin, and M. Dong, "Adaptive neural network control for active suspension system with actuator saturation," *IET Control Theory & Applications*, vol. 10, no. 14, pp. 1696–1705, Sep. 2016, doi: 10.1049/iet-cta.2015.1317.

[12] J. Chen, W. Liu, R. Ding, D. Sun, and R. Wang, "Reference model-based backstepping control of semi-active suspension for vehicles equipped with non-pneumatic wheels," *Machines*, vol. 13, no. 6, p. 476, May 2025, doi: 10.3390/machines13060476.

[13] H. Shi, J. Zeng, and J. Guo, "Disturbance observer-based sliding mode control of active vertical suspension for high-speed rail vehicles," *Vehicle System Dynamics*, vol. 62, no. 11, pp. 2912–2935, Nov. 2024, doi: 10.1080/00423114.2024.2305296.

[14] L. V. Meetei and D. K. Das, "Enhanced nonlinear disturbance observer based sliding mode control design for a fully active suspension system," *International Journal of Dynamics and Control*, vol. 9, no. 3, pp. 971–984, Sep. 2021, doi: 10.1007/s40435-020-00682-3.

[15] C. Niu, X. Liu, X. Jia, B. Gong, and B. Xu, "Active hydro-pneumatic suspension active disturbance rejection sliding mode control for improved vehicle stability," *SAE Technical Paper, SAE India Mobility Conference 2024*. SAE Technical Paper, SAE India Mobility Conference 2024, Dec. 05, 2024. doi: 10.4271/2024-28-0215.

[16] A. Azizi and H. Mobki, "Applied mechatronics: designing a sliding mode controller for active suspension system," *Complexity*, vol. 2021, no. 1, Jan. 2021, doi: 10.1155/2021/6626842.

[17] C. Ozbek, R. Burkan, and N. Yagiz, "Robust control of vehicle suspension systems with friction non-linearity for ride comfort enhancement," *Journal of Vibration and Control*, vol. 30, no. 5–6, pp. 1326–1338, Mar. 2024, doi: 10.1177/10775463231162133.

[18] N. S. Bajaba, "Ellipsoidal-based robust control for vehicle active suspension systems under load uncertainties and network-induced interruptions," *Reports in Mechanical Engineering*, vol. 6, no. 1, pp. 46–54, 2025, doi: 10.31181/rme442.

[19] Y. Yin, B. Luo, H. Ren, Q. Fang, and C. Zhang, "Robust control design for active suspension system with uncertain dynamics and actuator time delay," *Journal of Mechanical Science and Technology*, vol. 36, no. 12, pp. 6319–6327, Dec. 2022, doi: 10.1007/s12206-022-1143-1.

[20] T. Abut, E. Salkim, and H. Tugal, "Active suspension control for improved ride comfort and vehicle performance using HHO-based type-I and type-II fuzzy logic," *Biomimetics*, vol. 10, no. 10, p. 673, Oct. 2025, doi: 10.3390/biomimetics10100673.

[21] L. Ovalle, H. Ríos, and H. Ahmed, "Robust control for an active suspension system via continuous sliding-mode controllers," *Engineering Science and Technology, an International Journal*, vol. 28, p. 101026, Apr. 2022, doi: 10.1016/j.jestch.2021.06.006.

[22] J. B. Kimball, B. DeBoer, and K. Bubbar, "Adaptive control and reinforcement learning for vehicle suspension control: A review," *Annual Reviews in Control*, vol. 58, p. 100974, 2024, doi: 10.1016/j.arcontrol.2024.100974.

[23] Q. Zeng and J. Zhao, "Adaptive switching control of active suspension systems: a switched system point of view," *IEEE Transactions on Control Systems Technology*, vol. 32, no. 2, pp. 663–671, Mar. 2024, doi: 10.1109/TCST.2023.3318350.

[24] T. Shaqarin and B. R. Noack, "Enhancing mechanical safety in suspension systems: harnessing control Lyapunov and barrier functions for nonlinear quarter car model via quadratic programs," *Applied Sciences*, vol. 14, no. 8, p. 3140, Apr. 2024, doi: 10.3390/app14083140.

[25] R. Bai and D. Guo, "Sliding-mode control of the active suspension system with the dynamics of a hydraulic actuator," *Complexity*, vol. 2018, no. 1, Jan. 2018, doi: 10.1155/2018/5907208.
[26] C. A. Kedir and C. M. Abdissa, "PSO based linear parameter varying-model predictive control for trajectory tracking of autonomous vehicles," *Engineering Research Express*, vol. 6, no. 3, p. 035229, Sep. 2024, doi: 10.1088/2631-8695/ad722e.
[27] E. A. Teklu and C. M. Abdissa, "Genetic algorithm tuned super twisting sliding mode controller for suspension of Maglev train with flexible track," *IEEE Access*, vol. 11, pp. 30955–30969, 2023, doi: 10.1109/ACCESS.2023.3262416.
[28] A. A. Kolesnikov *et al.*, "Synergetic methods of complex systems control: mechanical and electromechanical systems," *Moscow: URSS*, 2006.
[29] A. A. Kolesnikov, A. A. Kuz'menko, and G. E. Veselov, *New design technology of modern control systems for the generation of electricity*. Moscow: Publishing House, 2011.
[30] T. Kumsaen, S. Simatrang, A. Boonyaprapasorn, and T. Sethaput, "Terminal synergetic controller for car's active suspension system using dragonfly algorithm," *Proceedings of International Conference on Artificial Life and Robotics*, vol. 29, pp. 1051–1055, Feb. 2024, doi: 10.5954/ICAROB.2024.GS6-4.
[31] D. N. Nguyen and T. A. Nguyen, "Proposing an original control algorithm for the active suspension system to improve vehicle vibration: Adaptive fuzzy sliding mode proportional-integral-derivative tuned by the fuzzy (AFSPIDF)," *Heliyon*, vol. 9, no. 3, p. e14210, Mar. 2023, doi: 10.1016/j.heliyon.2023.e14210.
[32] J. Thiyagarajan, P. Sathishkumar, and T. Muthuramalingam, "Experimental investigation of active suspension force control of electric motor driven actuator with estimation and tracking control strategy," *Materials Today: Proceedings*, vol. 90, pp. 279–286, 2023, doi: 10.1016/j.matpr.2023.07.311.
[33] R. Gamage, C. Rathnayake, R. Kalubowila, and S. Thilakarathne, "Design and development of a quarter-car model active suspension system for a mobile robot to enhance terrain adaptability with better stability and mobility," *Journal of Mechatronics and Robotics*, vol. 8, no. 1, pp. 39–48, Jan. 2024, doi: 10.3844/jmrsp.2024.39.48.

BIOGRAPHIES OF AUTHORS

Dao Trong Dung is currently a research associate at the Institute of Mechanical Engineering, Hanoi. He received his Bachelor's degree in automation engineering from Le Quy Don Technical University, Hanoi, in 2020, and is currently pursuing a Master's degree in automation engineering at the same university. His research interests include nonlinear control, embedded systems, measurement, and computer-based control. He can be contacted at daotrongdung0510@gmail.com.

Trong Nghia Le received his B.S. and M.S. degrees in electrical engineering from Le Quy Don Technical University, Hanoi, Vietnam, in 2003 and 2009, respectively. From 2004 to 2008, he served as a lecturer at Le Quy Don Technical University, where he was responsible for teaching digital signal processing and network integrated circuit design. He received his Ph.D. degree in engineering science from the National Cheng Kung University, Tainan, Taiwan, in 2015. Since 2015, he has been a researcher at the Center for Technical Quality Assurance and Technology Transfer, Le Quy Don Technical University. His research interests include nonlinear control, intelligent control, and embedded systems. He can be contacted at Nghiahp79@gmail.com.

Alexandr D. Lukyanov was born in 1970. He graduated from Moscow Institute of Physics and Technology in 1994, and defended his Ph.D. thesis in automation technology and equipment for mechanical and physical-technical processing in Don State Technical University, Russia in 1998. From 2008 to 2015 he was the Chief of Science Department of DSTU. From 2015 to the present, he is a Head of Chair "Automatization of production processes" of DSTU. His research interests include nonlinear dynamic, mathematical modeling, embedded systems, sensors and control. He can be contacted at alukjanov@donstu.ru.

Nguyen Xuan Chiem was born in 1983. He received a Ph.D. degree in Technology and equipment for mechanical and physical-technical processing from Don State Technical University, Russia in 2012. From 2013 to the present, he is a lecturer at the Department of Automation and Computing Techniques in the Institute of Control Engineering, Le Quy Don Technical University. His research interests include nonlinear control, intelligent control, and embedded systems. He can be contacted at chiemnx@mta.edu.vn.